Chinese Chemical Letters 36 (2025) 110601

Contents lists available at ScienceDirect

Chinese Chemical Letters

journal homepage: www.elsevier.com/locate/cclet

High-efficiency exudates drainage of anti-adhesion dressings for chronic wound

Bingyang Lu[a], Dehui Wang[a,*], Junchang Guo[a], Yang Shen[a], Qian Feng[b], Jinlong Yang[a], Xiao Han[a], Huali Yu[a], Luohuizi Li[a], Jiaxin Liu[a], Jing Luo[a,*], Huan Liu[b,*], Zhongwei Zhang[b,*], Xu Deng[a,c,*]

[a] Institute of Fundamental and Frontier Sciences, University of Electronic Science and Technology of China, Chengdu 610054, China
[b] Department of Critical Care Medicine, West China Hospital of Sichuan University, Chengdu 610041, China
[c] Shenzhen Institute for Advanced Study, University of Electronic Science and Technology of China, Shenzhen 518110, China

ARTICLE INFO

Article history:
Received 22 September 2024
Revised 27 October 2024
Accepted 31 October 2024
Available online 1 November 2024

Keywords:
Superhydrophobic-hydrophilic
Biological fluids repelled
Anti-adhesion and secondary trauma prevention
Exudates transport
Chronic wound healing treatment

ABSTRACT

Secondary trauma, resulting in undesirable injury and bleeding during wound dressing treatment, which will cause the treatment of chronic wounds ineffective. The medical cotton gauzes often bring strong adhesion due to the exudates absorbed and clots formed. Conversely, the easily detachable wound dressings neglect the wound seepage management, rendering them ineffective in facing the complexities of chronic wounds. To address this challenge, we propose a novel draining anti-adhesion dressings (DAD) by constructing the hydrophilic microchannels array on the superhydrophobic dressing. The superhydrophobic areas facilitate stable wound fluid repellence leading to achieve the anti-adhesion (18.7% detachment energy of cotton) and the microchannel array ensures the transportation of excess exudates (>92%) by the capillary force. Notably, our dressing demonstrates a significant healing-promoting in a chronic wound model in rats. The development of such dressings holds promise for advancing wound care practices and addressing the unique challenges posed by chronic wounds, offering a valuable solution for improved clinical outcomes.

Secondary trauma results undesirable bleeding and injury during wound treatments, affects the normal healing process of the wound, especially in chronic wounds for its challenging healing process which poses significant health issues in clinical settings, particularly for individuals with vulnerable skin, such as older people or those with underlying diseases [1]. The secondary trauma of chronic wounds make the treatment of chronic wounds to be meaningless, which bring more pain to patients.

The surface wettability of wound dressings usually affects the wetting behavior of biological fluids around the wound, which has an important influence on wound healing [2]. Traditional gauze dressings are easy to be soaked by biological fluids so that the wound fluid is absorbed by the wound dressings, but it will form a solid clot-gauze complex, which will often tear the wound when it is removed, causing secondary bleeding and trauma, which is not conducive to normal wound healing. Whereas the superhydrophobic surface brings a turning point to face the secondary trauma, due to its unique Cassie-Baxter state [3–6]. In this state, the phase separation of solid-air-liquid on the superhydrophobic surface can be easily peeled off from the skin due to the low adhesion area between the clot and the dressing [7]. Based on it, a kind of superhydrophobic hemostatic nanofiber composites were designed for minimal adhesion and showed a great effect in preventing secondary trauma [8,9].

However, the superhydrophobic dressing is powerless to absorb excess wound fluid, so the accumulation of wound fluid causes the risk of wound infection and wound soaking. And the continuous seepage of wound fluid is one of the primary reasons for the difficulty in healing chronic wounds, which becomes the breeding ground for bacteria and causes persistent chronic inflammation. Although a small amount of wound fluid has a positive effect on the healing of chronic wounds, but the ongoing issue of excessive wound seepage can negatively impact the wound repair process, leading to skin immersion, potential wound reinfection and patient discomfort [10–13]. Therefore, the management of wound fluids around the wound is a prerequisite for chronic wound healing [14–18]. Consequently, there is an urgent need to strike a bal-

* Corresponding authors.
E-mail addresses: wangdehui@uestc.edu.cn (D. Wang), luojing115@uestc.edu.cn (J. Luo), liuhuan881129@163.com (H. Liu), 716461751@qq.com (Z. Zhang), dengxu@uestc.edu.cn (X. Deng).

https://doi.org/10.1016/j.cclet.2024.110601
1001-8417/

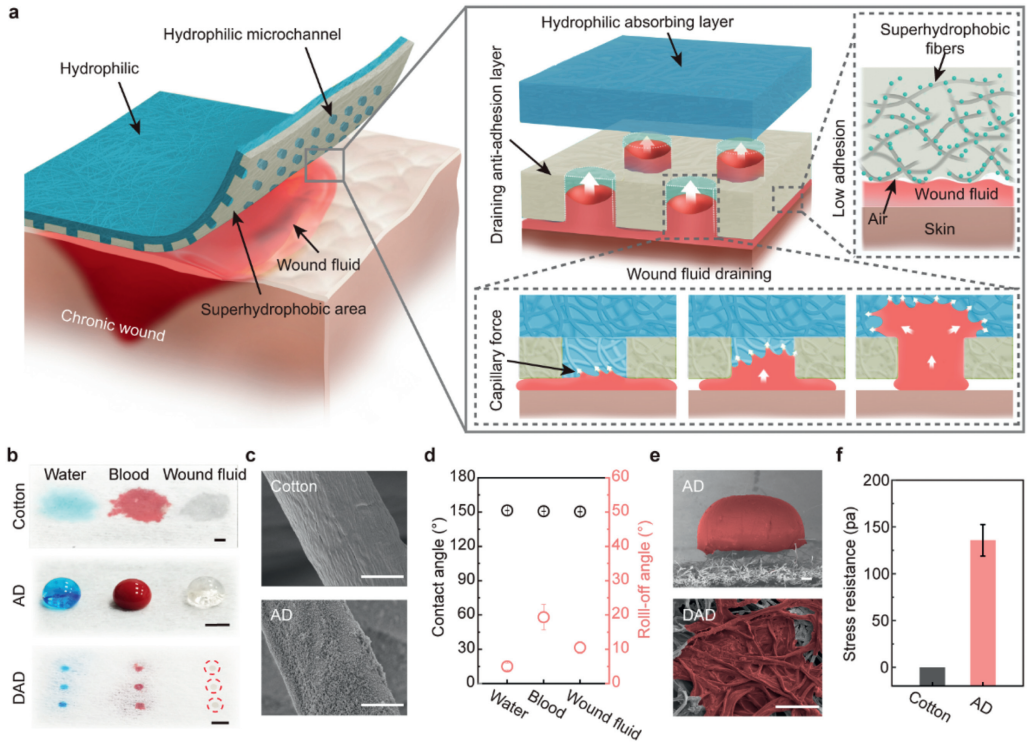

Fig. 1. Design of the draining anti-adhesion dressing (DAD) for treating chronic wounds. (a) Schematic of draining anti-adhesion dressing. (b) Images of cotton, superhydrophobic anti-adhesion wound dressing (AD), DAD, and the liquid added on them (Scale bar = 2 mm). (c) SEM images of conventional cotton and AD (Scale bar = 5 μm). (d) CA and RA of the water, blood, and wound fluid ($n = 5$). (e) SEM images of blood wetting the DAD and blood repelled by AD (Scale bar = 200 μm, blood wetting region dyed red). (f) Blood stress resistance ability of the cotton and AD ($n = 3$).

ance between minimizing secondary trauma and managing excessive wound seepage to facilitate the promotion of chronic wound healing.

Here, we report a draining anti-adhesion dressing (DAD) with high-efficiency exudates transport capacity, to manage the wound fluid and prevent secondary trauma by the arrangement of the hydrophilic microchannels on the superhydrophobic dressings (Fig. 1a). The non-wetting areas of the DAD with the stable wound fluid repellency, and the hydrophilic microchannels of the DAD presents the high-efficiency exudates draining driven by the capillary force. We carefully arranged the hydrophilic microchannel arrays to balance the relationship between anti-adhesion and liquid drainage, so that the DAD exhibited low peel strength when wound dressing was removed and desirable exudates management. This strategy accomplishes the regulation of excessive exudates and prevents secondary trauma, ultimately fostering the healing of chronic wounds, and promises to provide an effective solution for the secondary trauma prevention of chronic wounds in clinical.

As shown in Fig. 1a, the DAD consists of two layers, the bottom layer touches the wound required to be a superhydrophobic layer with uniformly distributed hydrophilic microchannels, and the top layer is untreated gauze for draining and storage excessive exudates (Fig. 1b). For the anti-adhesion capacity, a simple method that easy to achieve superhydrophobicity with large-area is employed and the detailed is shown in methods section.

Briefly, the conventional cotton fibers were coated with a dense layer of hydrophobic nanoparticles to reduce the surface energy while increasing the roughness (Fig. 1c), obtaining an anti-adhesion dressing (AD) with outstanding liquid repellency. It demonstrated the non-wettability with contact angle (CA) $> 150°$ and roll-off angle (RA) $\approx 10°$, which was measured by using the water, blood and the wound fluid as the measurement liquid, respectively (Fig. 1d). Optimal preparation technology facilitated the slipping of blood from the AD after 2 h (Figs. S1-S3 in Supporting information), and the hydrophobic SiO_2 nanoparticles adhered on fibers steadily without affecting the breathability (Figs. S4 and S5 in Supporting information) [19]. When blood clotting naturally on both cotton and AD, the fibers of AD demonstrated exceptional blood-repelling ability. Only some fibers supported the blood clot without wetting the AD, maintaining the liquid in a Cassie state (Fig. 1e), and the protein adhesion was approximately 77 times smaller than cotton (Fig. S6 in Supporting information). Consequently, the blood clot could be easily separated from the AD with a light force (14.9 ± 7.2 mN) for the air trapped between the solid surface and the liquid reduces the contact area with blood clot [11], and the fibers did not experience any traction during this separation process. In contrast with conventional cotton gauzes, the clot was coagulated with the fibers, requiring a heavy force (443.1 ± 50.0 mN) for the separation (Fig. S7 in Supporting information). The significant reduction in solid-liquid contact area due to superhydrophobic modification indicated that AD possessed sustained blood-repelling ability and low clot peeling force, making it suitable for the preparation of DAD. For evaluation of the liquid pressure resistance of the non-wetting state, and the simply selective infiltration, the AD exhibited blood stress resistance of 136.6 ± 14.9 Pa compared to the conventional cotton (Fig. 1f).

For the exudates transport capacity, the hydrophilic microchannel array was constructed by plasma activation under mask plates, and DAD could be easily prepared using commercial dressings (Figs. S8-S10 in Supporting information) [20], and the blood was only wetting the hydrophilic microchannels of DAD (Fig. 1e). To prevent the reverting to a hydrophobic state of the hydrophilic fibers in microchannel, a hydrophilic polymer solution, such as polyethylene glycol (PEG) was coated on the fiber in microchannel to enable long-term storage and use for its good biocompatibility [21,22].

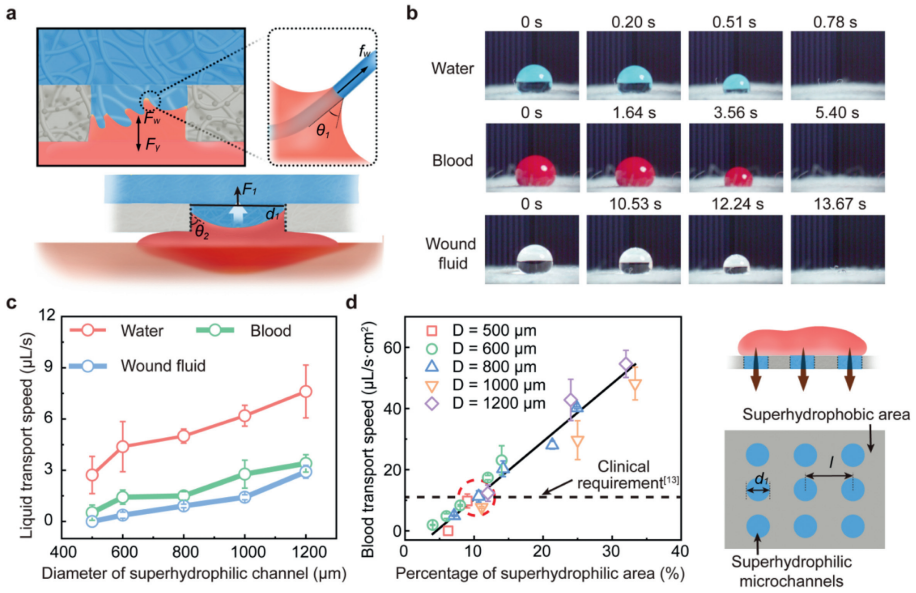

Fig. 2. The exudates draining regulation by hydrophilic microchannels of the anti-adhesion dressing. (a) Theoretical model of the liquid transport through the wound dressing on the wound. (b) Images of the different liquids transport through the hydrophilic microchannel. (c) The speed of different liquids transport through the single hydrophilic microchannel ($n = 3$). (d) The blood transport speed through the hydrophilic area comprised of various hydrophilic microchannels ($n = 3$, the red dotted circle including the 10% hydrophilic proportion of DAD with different hydrophilic microchannel diameters, and the black line represented the positively correlated).

According to Laplace pressure and the capillarity model [23,24], the efficient expulsion of liquid depends on the capillarity to actuate, and the liquid transport process module is shown in Fig. 2a, and the total actuated force (F_ω) followed Eq. 1, which could reflect the wetting of the hydrophilic channel

$$F_\omega \sim 2d_1k^2\gamma\cos\theta_1\cos\alpha \quad (1)$$

where γ is the interfacial tension of the liquid, θ_1 is Young's equilibrium contact angle of the cotton fiber coating by hydrophilic polymer, k is constant to reflect the density of the cotton, the d_1 is the diameter of the hydrophilic channel, and α is the angle to correct the direction for analyzing the exported ability only, it can easily get that F_ω is positively correlated with d_1 for same liquid. Then, the way of creating the hole in the hydrophilic channel proved to be advantageous for liquid transport because of reduced flow resistance (Fig. S11 in Supporting information).

Next, the liquid is exported through the hydrophilic channel. The influencing factor on the force is the capillary force (F_c) required for contact with the absorbed layer [25], which can be quantified as Eq. 2. Where the θ_2 is Young's equilibrium contact angle of the absorbing layer, and the F_c is also dependent on the d_1 with the same absorbing layer.

$$F_c \sim \pi d_1\gamma\cos\theta_2 \quad (2)$$

To further verify the theoretical model, the passage of liquid (5 μL water, blood, wound fluid) through the hydrophilic channel was recorded by high-speed camera (Figs. 2b and c, Figs. S12-S14 in Supporting information). Overall, the wetting time (from initial contact with the liquid to the start of transmission) was used to evaluate the duration from liquid contact to the beginning of transportation, and it depended on F_ω. It showed that the time of wetting gradually increased with larger hydrophilic channel diameters (d_1), which confirmed the correctness of Eq. 1 in the theoretical model. Additionally, the total time for the entire liquid expulsion process depended on F_c, which indicated that larger hydrophilic channels facilitated quicker liquid transport, confirming the validity of Eq. 2. Furthermore, the transport speed of the microchannel was assessed by designing the percentage of hydrophilic area through the regulation of channel diameter and spacing. As shown in Fig. 2d, the transport speed exhibited a positive correlation with the hydrophilic area. Considering the ideal mass seepage of chronic wounds (0.12 μL/s) [26], it was hypothesized that approximately 10% hydrophilic area would be sufficient for transporting wound fluid (the dotted line represented the 100 times). For assessed blood exported rate *in vitro*, the DAD could reach blood export efficiency of 92% (Fig. S15 in Supporting information).

The introduction of hydrophilic channels inevitably impacts the peeling force of AD and the peeling force curve elucidated that the presence of a clot on the hydrophilic channel precipitates a force increase, but it was significantly lower compared to the cotton, attributed to its adherence solely in micro-sized clots (Fig. 3a). A visual representation of the peeling process from pigskin *in vitro* was provided in Fig. S16 (Supporting information).

In the capillary force liquid-exported theoretical model of DAD, the d_1 played a crucial role, at the same time, it also had a strong correlation with the peeling force (F_p) as indicated by $F_p \sim {d_1}^2$. Consequently, there are two principles to arrange the microchannel array of DAD. On the one hand, the clot adherence to the skin for each hydrophilic channel was examined by designing a single row DAD, revealing the influence of channel diameter on peeling. The peeling force curve indicated that a larger channel diameter corresponded to a higher peeling force, and a higher peeling force implied greater difficulty in separating the wound from the skin, al nigning with the theoretical model (Fig. S17 in Supporting information). Considering the delicate balance between liquid-exported and wound dressing removal, about 800 μm might be a suitable diameter for hydrophilic channels designed on DAD (Fig. 3b). On the other hand, the hydrophilic channel was designed as the array adhered to pigskin, with the hydrophilic area maintained at approximately 10% (red dotted circle in Fig. 2d), through adjustments in the diameter and number of channels to influence the concentration and dispersion of force. The peeling process was concretely defined as relieving pain in comparison to cotton (Fig. 3c and Fig. S18 in Supporting information). The results demonstrated that the introduction of micro-sized channels could reduce the pain sensation to approximately 3 times, the detachment energy of DAD could reduce to 18.7%. And larger-sized hydrophilic channels were observed to amplify pain during the peeling process, while nu-

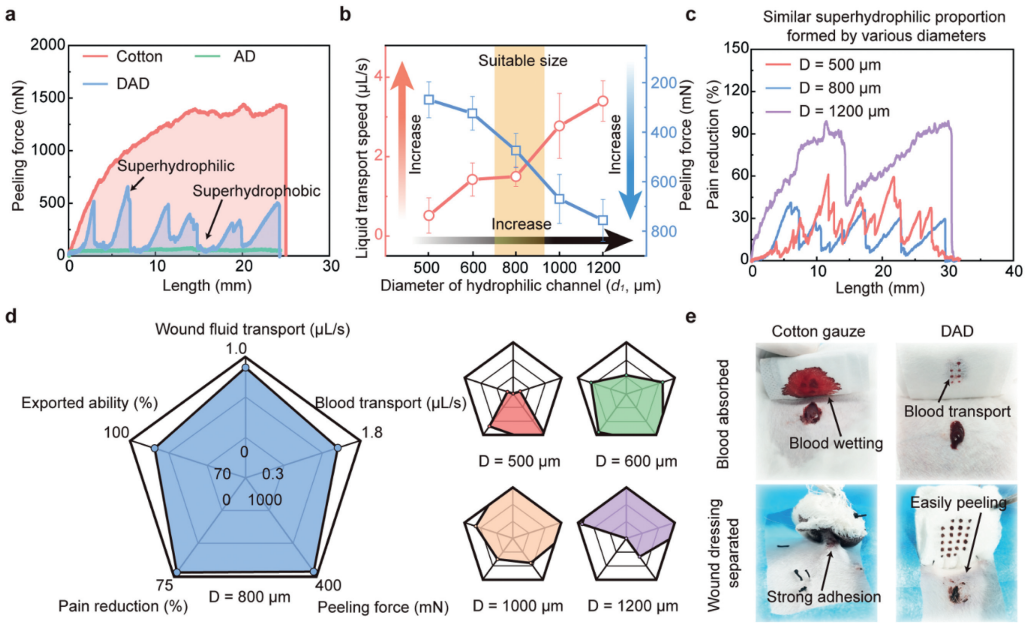

Fig. 3. The microarray arrangement guidance the anti-adhesion property for preventing secondary trauma. (a) The peeling force curve of various wound dressings from pigskin. (b) The balance of liquid transport rate and peeling force for various sizes of hydrophilic microchannels. (c) The peeling force curve for various sizes of hydrophilic microchannels as array (about 10% hydrophilic proportion) from pigskin. (d) The radar chart to evaluate the diameter of the channel on the wound dressings. (e) Images of wound dressing used and removed in abdominal vein wound of rabbits.

merous small hydrophilic channels also induced a high degree of pain. This phenomenon was attributed to the simultaneous tearing of numerous hydrophilic regions in contact with the skin, leading to an increased disengagement line, and the pain intensity was quantified by comparison with cotton (Fig. S18f) [27,28]. Further, a comprehensive analysis was undertaken to establish criteria for the hydrophilic channel diameter, including the speed of blood and wound fluid transport, peeling force, pain reduction, and liquid transport capability (Fig. 3d). The findings revealed that DAD exhibited superior comprehensive abilities when the channel diameter was set at about 800 μm, and about 600 μm channel on DAD emerged as a favorable choice for small amount of exudate.

The separation between the skin and the wound dressing was visually demonstrated *in vivo* (Fig. 3e and Fig. S19 in Supporting information). When the DAD was applied to the abdominal vein wound of New Zealand white rabbits, both the cotton and DAD demonstrated the capability to transport blood to the absorbent layer (Movies S1 and S3 in Supporting information). Accumulation of blood on the wound surface occurred as AD repelled the blood (Movie S2 in Supporting information). After 2 h, the wound dressing was peeled off, revealing that peeling the cotton resulted in the wound reopening, whereas the DAD group exhibited an intact blood clot. In contrast, wounds treated with AD exhibited strong adhesion, attributed to the excessive blood, causing it to assume the Wenzel state and making detachment challenging [29].

In the wound region, the fibroblast cells, human venous endothelial cells (HUVEC), and macrophages (MA, RAW 267.4) played physiological roles in wound repair [30,31]. Cells selectively adhered only to the activated hydrophilic channel due to hydrophilic and superhydrophobic transformation (Fig. S20 in Supporting information). The CCK-8 and Calcein AM/PI staining results proved that DAD had good biocompatibility (Figs. S21-S26 in Supporting information). The biosafety of DAD ensured that the superhydrophobic construction was fluoride-free [32]. Moreover, compared with hydrophilic wound dressing, superhydrophobic dressing possesses antibacterial adhesion properties, especially the HACC (chitosan quaternary ammonium salt) can also be adsorbed in hydrophilic channels as an antibacterial material (Figs. S27-S29 in Supporting information). And the DAD also had a good hemocompatibility (Fig. S30 in Supporting information).

Clinical chronic wounds can arise from various reasons with wound exudate, including infected wounds, diabetic wounds, pressure ulcers, and so on. A pressure ulcer wound model was created by applying persistent pressure with a magnet [33], and a mass of wound fluid began to appear at day 5 (Fig. 4a and Fig. S31 in Supporting information). At day 7, the magnet was removed, and the pressure ulcer was treated with the wound dressing. It was observed that the wound exhibited accelerated healing directly following treatment with DAD (Fig. 4b). After comparison with the control group, DAD significantly promoted pressure ulcer healing as a wound dressing, demonstrating a repair rate approximately 2-3 times higher than that of conventional cotton (Fig. 4d). At day 20, HE staining of the wound revealed clot and incomplete epidermis, except for the wound treated with DAD (Fig. 4c). Though the comprehensive analysis including wound situation, the formation of new blood vessels, the thickness of the epidermis, and the collagen volume fraction (CVF) showed that the wound treated with DAD had a mature and optimal wound status (Fig. 4c and Fig. S32c in Supporting information) [34,35]. To investigate the underlying reasons for the promotion of chronic wound healing by DAD, the inflammatory response in the early stages of chronic wounds was studied through staining with CD68/CD206. The results revealed the M2 phenotype predominated with DAD-treated, which exhibited approximately three times more than others (Figs. 4c and e, Fig. S32a in Supporting information) [36,37]. This indicated that the inflammatory response in chronic wounds was regulated by DAD treatment in the management of excess wound seepage, thereby facilitating quick healing of chronic wounds. Moreover, the same wound dressing was applied to normal acute wounds, which exhibited no significant treatment (Fig. S33 in Supporting information).

Simultaneously, to conclusively validate the results, infected wound, and diabetic wound models were established to observe the healing process. In essence, DAD also facilitated the healing

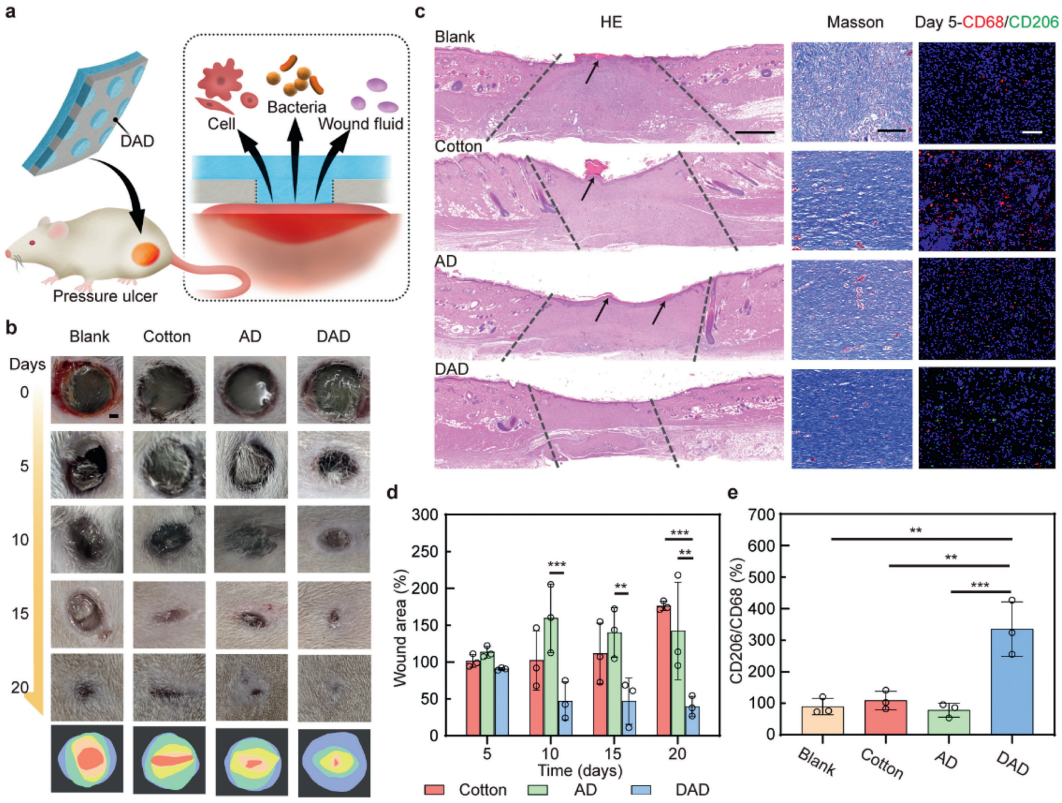

Fig. 4. The pressure ulcer healing with draining anti-adhesion dressing. (a) Schematic of the wound dressings used to heal the pressure ulcer wound. (b) Images of pressure ulcer wound healed with different wound dressing at day 5, 10, 15, 20 (Scale bar = 1 mm). (c) The HE (Scale bar = 1000 μm) and Masson (Scale bar = 100 μm) staining of the wound at day 20, and the CD68/CD206 (red/green) staining of the wound at day 5 (Scale bar = 100 μm) ($n = 3$, the black arrow showed the unhealing epidermis). (d) The wound healed area compared with the blank group at day 5, 10, 15, 20 ($n = 3$). (e) The fluorescence area of CD206/CD68 at day 5 ($n = 3$, $^{**}P < 0.01$, $^{***}P < 0.001$).

of infected wounds (Figs. S34 and S35 in Supporting information) and diabetic wounds (Figs. S36 and S37 in Supporting information), by effectively managing wound seepage to regulate inflammation. Thus, DAD specifically regulated wound seepage to reduce inflammation in chronic wounds, bringing the wound closer to a healthy tissue state.

In summary, based on the need to prevent secondary trauma, the draining anti-adhesion dressings (DAD) with high-efficiency exudates transport capacity were developed in this work through the superhydrophobic/hydrophilic pattern, and the hydrophilic microchannels array was carefully designed through regulating the diameter and distribution of microchannels, to balance the relationship between anti-adhesion and liquid drainage. The DAD showed the good biocompatibility and promotion healing of chronic wounds, which integrated holds promise for addressing the challenges associated with the impaired healing and secondary trauma of chronic wounds in clinical settings. With further development and clinical testing, the strategic approach to wound dressing design outlined in this study holds significant promise.

Declaration of competing interest

The authors declare that they have no known competing financial interests or personal relationships that could have appeared to influence the work reported in this paper.

CRediT authorship contribution statement

Bingyang Lu: Writing – review & editing, Writing – original draft, Visualization, Validation, Methodology, Investigation, Formal analysis, Data curation, Conceptualization. **Dehui Wang:** Writing – review & editing, Supervision, Resources, Funding acquisition. **Junchang Guo:** Visualization, Conceptualization. **Yang Shen:** Visualization, Methodology. **Qian Feng:** Investigation. **Jinlong Yang:** Visualization. **Xiao Han:** Visualization. **Huali Yu:** Methodology. **Luohuizi Li:** Methodology. **Jiaxin Liu:** Methodology. **Jing Luo:** Writing – review & editing, Visualization, Funding acquisition, Conceptualization. **Huan Liu:** Writing – review & editing, Visualization, Investigation. **Zhongwei Zhang:** Writing – review & editing, Visualization, Investigation. **Xu Deng:** Writing – review & editing, Visualization, Validation, Supervision, Resources, Funding acquisition, Conceptualization.

Acknowledgments

The authors acknowledge funding support by the National Nature Science Foundation of China (Nos. 22275028, 22325201, 52103136 and 22205033), the Shenzhen Science and Technology Program (No. JCYJ20210324142210027), the Sichuan Outstanding Young Scholars Foundation (No. 2021JDJQ0013), the Sichuan Science and Technology Program (No. 2023JDRC0081), and the Fundamental Research Funds for the Central Universities (Nos. ZYGX2021YGCX009 and ZYGX2021YGLH207).

Supplementary materials

Supplementary material associated with this article can be found, in the online version, at doi:10.1016/j.cclet.2024.110601.

References

[1] V. Falanga, R.R. Isseroff, A.M. Soulika, et al., Nat. Rev. Dis. Primers 8 (2022) 50.
[2] B. Xu, A. Li, R. Wang, et al., Adv. Funct. Mater. 31 (2021) 2105265.
[3] V. Jokinen, E. Kankuri, S. Hoshian, S. Franssila, R.H.A. Ras, Adv. Mater. 30 (2018) 1705104.

[4] E.J. Falde, S.T. Yohe, Y.L. Colson, M.W. Grinstaff, Burns Trauma 104 (2016) 87–103.
[5] S. Movafaghi, W. Wang, D.L. Bark, et al., Mater. Horiz. 6 (2019) 1596–1610.
[6] J. Luo, H.L. Yu, B.Y. Lu, D.H. Wang, X. Deng, Small Methods 6 (2022) 2201106.
[7] D.H. Wang, Q.Q. Sun, M.J. Hokkanen, et al., Nature 582 (2020) 55–59.
[8] Z. Li, A. Milionis, Y. Zheng, et al., Nat. Commun. 10 (2019) 5562.
[9] Y. Li, F. Niu, X.T. Zhao, C.H. Yap, Z. Li, Adv. Mater. Interfaces 8 (2021) 2101412.
[10] E. Eriksson, P.Y. Liu, G.S. Schultz, et al., Wound Repair Regen. 30 (2022) 156–171.
[11] G. Han, R. Ceilley, Adv. Ther. 34 (2017) 599–610.
[12] M. Minsart, S. Van Vlierberghe, P. Dubruel, A. Mignon, Burns Trauma 10 (2022) tkac024.
[13] Y.N. Zhu, J.M. Zhang, J.Y. Song, et al., Adv. Funct. Mater. 30 (2020) 1905493.
[14] L.X. Shi, X. Liu, W.S. Wang, L. Jiang, S.T. Wang, Adv. Mater. 31 (2019) 1804187.
[15] W.Y. Xiao, X.Z. Wan, L.X. Shi, et al., Adv. Mater. 36 (2024) 2401539.
[16] L.B. Zhou, F. Liu, J.Y. You, et al., Adv. Healthc. Mater. 13 (2023) 2303460.
[17] Z. Xu, J.L. Fan, W.G. Tian, et al., Adv. Funct. Mater. 34 (2024) 2307449.
[18] L.R. Wang, Y. Luo, Y.C. Song, et al., ACS Nano 18 (2024) 3468–3479.
[19] K. Nuutila, E. Eriksson, Adv. Wound Care 10 (2021) 685–698.
[20] K.M. Hotchkiss, G.B. Reddy, S.L. Hyzy, et al., Acta Biomater. 31 (2016) 425–434.
[21] L.W. Shi, J.Q. Zhang, M. Zhao, et al., Nanoscale 13 (2021) 10748–10764.
[22] S.H. Zhang, H. Zhou, C. Huang, et al., Chin. Chem. Lett. 33 (2022) 4321–4325.
[23] X.L. Tian, H. Jin, J. Sainio, R.H.A. Ras, O. Ikkala, Adv. Funct. Mater. 24 (2014) 6023–6028.
[24] L.P. Xu, B. Dai, J.B. Fan, et al., Nanoscale 7 (2015) 13164–13167.
[25] H.J. Butt, M. Kappl, Adv. Colloid Interface Sci. 146 (2009) 48–60.
[26] T.R. Shih, S. Park, L.R. Thorlacius, et al., Arch. Dermatol. Res. 315 (2023) 1863–1874.
[27] W. Yang, V.R. Sherman, B. Gludovatz, et al., Nat. Commun. 6 (2015) 6649.
[28] Z.M. Guo, R. Hakkou, J.G. Yang, Y.L. Wang, Colloid Surf. A: Physicochem. Eng. Asp. 615 (2021) 126041.
[29] H.Y. He, W.K. Zhou, J. Gao, et al., Nat. Commun. 13 (2022) 552.
[30] B.Y. Lu, X. Han, D. Zou, et al., Mater. Today Bio 16 (2022) 100392.
[31] X.L. Liang, C.L. Huang, H. Liu, et al., Chin. Chem. Lett. 35 (2024) 109442.
[32] K. Dec, A. Łukomska, D. Maciejewska, et al., Biol. Trace. Elem. Res. 177 (2017) 224–234.
[33] I. Stadler, R.Y. Zhang, P. Oskoui, M.S. Whittaker, R.J. Lanzafame, J. Invest. Surg. 17 (2004) 221–227.
[34] L. Zhou, H. Zheng, Z.X. Liu, et al., ACS Nano 15 (2021) 2468–2480.
[35] G. Theocharidis, H. Yuk, H. Roh, et al., Nat. Biomed. Eng. 6 (2022) 1118–1133.
[36] Y.J. Fu, Y.F. Shi, L.Y. Wang, et al., Adv. Sci. 10 (2023) 2206771.
[37] C.X. Tu, H.D. Lu, T. Zhou, et al., Biomaterials 286 (2022) 121597.